

Production Cross-sections for the Residual Radionuclides from the $^{nat}\text{Pd}(p,x)$ and $^{nat}\text{Cd}(p,x)$ Processes up to 40 MeV

Mayeen U. KHANDAKER, Kwangsoo KIM, Manwoo LEE, Kyungsook KIM, and Guinyun KIM *

Department of Physics, Kyungpook National University, Daegu 702-701, Korea

*) Contact information: Tel. +82(53)950-5320, E-mail: gnkim@knu.ac.kr

Abstract

Independent and cumulative production cross-sections of the $^{nat}\text{Cd}(p,x)^{109g,111g,114m}\text{In}$ and $^{nat}\text{Pd}(p,x)^{105}\text{Rh}$ nuclear processes have been reported from 40 MeV down to their threshold energy by using a stacked-foil activation technique combined with high purity germanium γ -ray spectrometry. Measured data were compared with the available literature data and the theoretical data from the model calculations by the TALYS and ALICE-IPPE codes. Integral yields were also deduced for all the measured radionuclides. The measured cross-sections have a significance for various practical applications; nuclear medicine, nuclear technology, radioactive waste handling etc.

Keywords: *Indium and Rhodium radionuclides, natural cadmium and palladium targets; 42 MeV proton; stacked-foil technique; excitation functions; medical applications.*

1. Introduction

The study of light ion-induced nuclear reactions leading to the production of various radionuclides is finding increasing importance for medical and technological applications. The versatile ion-accelerating machine cyclotrons are employed to produce these radionuclides. The physical basis of a radionuclide production could be optimized by using data on nuclear cross-sections. Therefore, excitation functions and/or nuclear cross-sections have great significance in the production and the quality control of desired radionuclides for various practical applications, especially in nuclear medicine [1].

Cadmium (Cd) and Palladium (Pd) are ideal target materials for the production of medically important radionuclides, such as $^{109,111,114m}\text{In}$, and ^{105}Rh , respectively. The radionuclide ^{111}In is widely used in diagnostic nuclear medicine [2]. The radionuclide ^{109}In is used for diagnostic purposes using PET. It is interesting to note that, ^{114m}In and its daughter radionuclide ^{114}In are usually regarded as undesirable long-lived impurities in ^{111}In -labeled radiopharmaceuticals for a diagnostic use. However, there is increasing interest in studying ^{114m}In to determine the long-term stability and bio kinetics of indium-labeled pharmaceuticals as well as for radionuclide therapy at a low-energy [3-4]. On the other hand, the ^{105}Rh radionuclide is a promising candidate for targeted radiotherapy [5-6]. The emission of beta ($E_{\beta^-} = 570 \text{ keV } 70\%, 250 \text{ keV } 30\%$) and γ -ray (318.9 keV 19%) with a moderate energy, and medium half-life (1.44 days) make this radionuclide attractive for the dosimetry and the pharmacokinetic perspective [6]. Currently, a large amount and a high specific activity ^{105}Rh radionuclide is produced by a nuclear reactor using an enriched ^{104}Ru target through the indirect $^{104}\text{Ru}(n,\gamma)^{105}\text{Ru} \rightarrow ^{105}\text{Rh}$ process. But, an unsolved problem with the current production methods is the high level of Ru impurity associated with the radiochemical separation method used [7]. It is also possible to obtain very large quantities of ^{105}Rh as a fission product, if required [8]. But, the radiochemical work involved in the separation of

fission products is rather cumbersome. However, alternatively this ^{105}Rh radionuclide can be produced in a no carrier added (NCA) form by a using medium energy cyclotron through the proton irradiations on a palladium target.

A general survey of the literature [1, 9-12] revealed that only a few earlier investigations have been carried out for the production of medically and technologically important radionuclides from a proton bombardment on natural and/or enriched Cd (or Pd) targets but considerable discrepancies are found among them. Therefore, new experimental data is required to reduce these discrepancies and also to prepare a recommended database for an optimal production of important radionuclides. Hence, we have measured the production cross-sections of residual radionuclides from the $^{\text{nat}}\text{Cd}(p,x)^{109\text{g},111\text{g},114\text{m}}\text{In}$ and $^{\text{nat}}\text{Pd}(p,x)^{105}\text{Rh}$ nuclear processes up to 40 MeV by using a stacked-foil activation technique and using an Azimuthally Field Varying (AVF) MC-50 cyclotron at the Korea Institute of Radiological and Medical Sciences (KIRAMS).

2. Experimental procedure

The irradiation technique, the activity determination and the data evaluation procedures were similar to our previous works [13]. Some important features relevant to this work are discussed as follows. A well established stacked-foil activation technique combined with a high-resolution γ -ray spectrometer was employed to determine the excitation functions of the $^{\text{nat}}\text{Cd}(p,x)^{109\text{g},111\text{g},114\text{m}}\text{In}$ and $^{\text{nat}}\text{Pd}(p,x)^{105}\text{Rh}$ nuclear processes. High purity Cd ($>99.98\%$, 50 μm thick) and Pd ($>99.99\%$, 50 μm thick) foils with natural isotopic composition was used as the targets for the irradiation. Several foils of copper (100 μm thick) and aluminum (100 μm thick) were also assembled in the stack to monitor the beam intensity and to degrade the beam energy, respectively. The stacked-foils were irradiated for 60 minutes by a proton energy of 42.1 MeV with a beam current of about 100 nA from an external beam line of the MC-50 cyclotron at the KIRAMS. The spectrum analysis was done using the Gamma Vision 5.0 (EG&G Ortec) program. The photo peak efficiency curve of the gamma spectrometer was calibrated with a set of standard point sources. The proton beam intensity was determined by using the monitoring reaction of $^{\text{nat}}\text{Cu}(p,x)^{62}\text{Zn}$ with known cross sections from the ref. [14]. The proton energy degradation along the stacked foils was calculated by using the computer program SRIM-2003 [15]. The activation cross-sections for the $^{\text{nat}}\text{Cd}(p,x)$ and $^{\text{nat}}\text{Pd}(p,x)$ processes were determined using a well-known activation formula [13]. The decay data of the radioactive products were taken from the NUDAT database [16], and presented in Table 1.

The uncertainty of the proton energy for each point were estimated from the uncertainty of the incident beam energy, the target thickness, and the beam straggling. On the other hand, the uncertainty of the cross-sections were estimated using the uncertainty propagation formula by considering the following uncertainties; statistical uncertainty of the γ -ray counting ($\sim 10\%$), uncertainty in the monitor flux ($\sim 7\%$), uncertainty in the detector efficiency ($\sim 4\%$), and so on. The overall uncertainties of the measured cross-sections were in the range of 8-15 %.

3. Theoretical calculations

The excitation functions of the $^{\text{nat}}\text{Cd}(p,x)^{109\text{g},111\text{g},114\text{m}}\text{In}$ and $^{\text{nat}}\text{Pd}(p,x)^{105}\text{Rh}$ nuclear processes at proton energies up to 100 MeV were theoretically calculated using the model calculations by the TALYS [17] and ALICE-IPPE [18] codes. In the case of the TALYS code, the present results were mostly evaluated using the default values of various models, but the very important inputs like the optical model parameters, discrete energy levels and level

densities of the nuclides involved in the calculations have been taken care of in a proper way during the calculations. Furthermore, the data of the ALICE-IPPE code were taken from the IAEA (www-nds.iaea.org), where it is compiled as the MENDL-2P database.

Table 1 Decay data for the $^{nat}\text{Cd}(p,x)$ and $^{nat}\text{Pd}(p,x)$ nuclear processes

Nuclei	Half-life $T_{1/2}$	Decay mode (%)	E_γ (keV)	I_γ (%)	Contributing reactions	Q-value (MeV)	Threshold (MeV)
^{109g}In	4.2 h	EC (100)	203.5	73.5	$^{110}\text{Cd}(p, 2n)$	-12.718	12.8347
			426.25	4.12	$^{111}\text{Cd}(p, 3n)$	-19.693	19.8729
			623.7	5.5	$^{112}\text{Cd}(p, 4n)$	-29.092	29.3542
			1149.1	4.3	$^{113}\text{Cd}(p, 5n)$	-35.632	35.9505
^{111g}In	2.81 d	EC (100)	171.28	90	$^{111}\text{Cd}(p, n)$	-1.6477	1.66276
			245.39	94	$^{112}\text{Cd}(p, 2n)$	-11.046	11.1454
					$^{113}\text{Cd}(p, 3n)$	-17.586	17.7432
					$^{114}\text{Cd}(p, 4n)$	-26.629	26.8646
^{114m}In	49.51 d	IT+EC (100)	190.29	14.74	$^{114}\text{Cd}(p, n)$	-2.2342	2.25401
			558.46		$^{116}\text{Cd}(p, 3n)$	-17.075	17.2238
^{105}Rh	1.47 d	β^- (100)	318.9	19.1	$^{106}\text{Pd}(p, 2p)$	-9.3470	9.4360
					$^{108}\text{Pd}(p, \alpha)$	3.18925	0.0
					$^{110}\text{Pd}(p, 2n\alpha)$	-11.781	11.889

4. Results and discussion

4.1 The $^{nat}\text{Cd}(p,x)^{109g}\text{In}$ processes

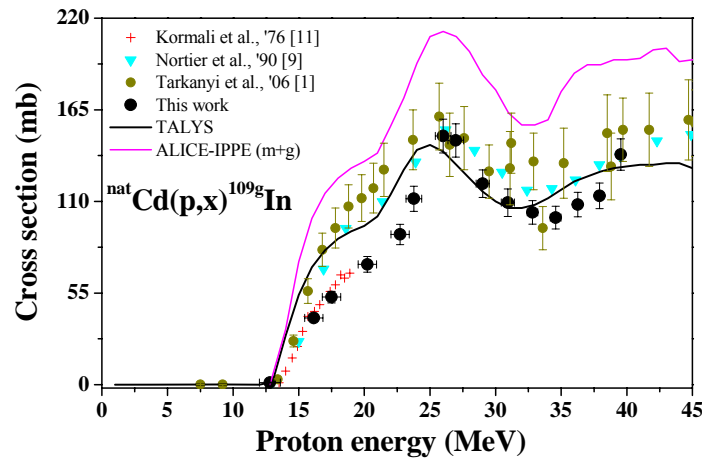


Fig. 1 Excitation function for the $^{nat}\text{Cd}(p,x)^{109g}\text{In}$ processes

^{109}In has one long-lived ground state radionuclide ^{109g}In ($T_{1/2}= 4.20$ h), and two short-lived excited state radioisomers ^{109m}In ($T_{1/2}= 1.34$ m) and ^{109n}In ($T_{1/2}= 0.21$ s). Both of the isomers completely decay to their ground state ^{109g}In through a 100% IT decay process. As the γ -ray counting process was started after a cooling time of about 1.5 h, the measured production cross-sections of the ^{109g}In radionuclide are considered as cumulative ones. The measured excitation function of the ^{109g}In is shown in Fig. 1 in comparison with the available literature data and the theoretical data by the model code calculations. The first maximum obtained at around 25 MeV signifies the direct contribution of the (p, 2n) and (p, 3n) reactions. The measured data revealed a very good agreement with the data reported by Kormali et al.

[11]. However, a good overall agreement, especially for the shape of the excitation function is obtained with the Nortier et al. [9], Tarkanyi et al. [1], and also with the theoretical data from the TALYS code for the whole investigated energy region. The ALICE-IPPE code predicted data with a similar shape for the measured excitation function, but overestimated the absolute values by about 20%.

4.2 The $^{nat}\text{Cd}(p,x)^{111g}\text{In}$ processes

^{111}In has a long-lived ground state radionuclide ^{111g}In ($T_{1/2}=2.80$ d) and a short-lived isomer ^{111m}In ($T_{1/2}=7.70$ m), whereas the isomeric state radionuclide completely decays to its ground state by an IT process. Therefore, the measured cross-sections of the ^{111g}In radionuclide is a cumulative one. The measured excitation function of ^{111g}In is shown in Fig. 2 together with the available literature values and the data from the model calculations. The formation of the ^{111g}In radionuclide is also contributed to by the direct reactions collected in Table 1. The contribution of the (p,n), (p,2n) and (p,3n) reactions formed a sharp maximum at around 24 MeV, whereas the second maximum at around 40 MeV is from the contribution of the $^{114}\text{Cd}(p,4n)$ reaction. The present results are in good agreement with the measured data reported by Tarkanyi et al. [1], Nortier et al. [9], and the deduced normalized values from the IAEA recommended data [19]. However, the data reported by Zaitseva et al. [10] is different from any other measurements. The data calculated by the TALYS and ALICE-IPPE codes revealed a good agreement for both the shape and magnitude with the measured data.

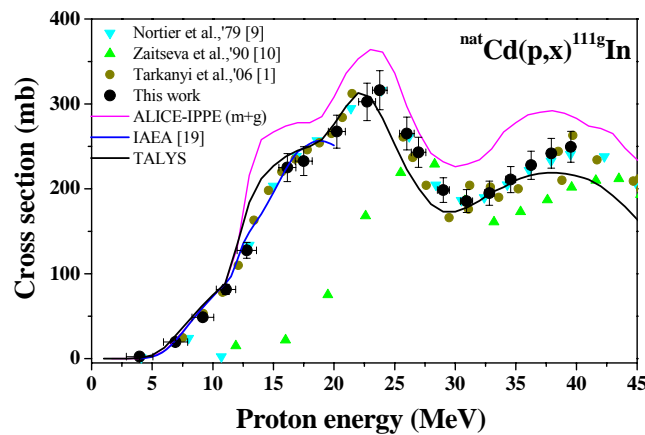


Fig. 2 Excitation function for the $^{nat}\text{Cd}(p,x)^{111g}\text{In}$ processes

4.3 The $^{nat}\text{Cd}(p,x)^{114m}\text{In}$ processes

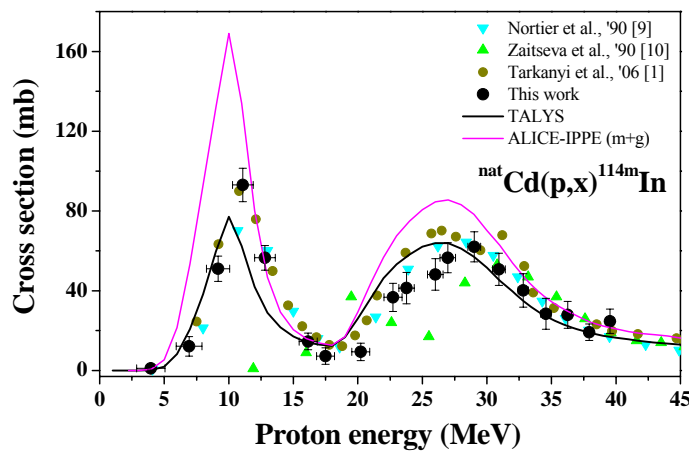


Fig. 3 Excitation function for the $^{nat}\text{Cd}(p,x)^{114m}\text{In}$ processes

Except for the short-lived ground state radionuclide ^{114g}In ($T_{1/2}= 1.20$ m), ^{114}In has two isomeric states ^{114m}In ($T_{1/2}= 49.51$ d) and ^{114n}In ($T_{1/2}= 0.0431$ s). Under the present experimental conditions, we could only measure the ^{114m}In radionuclide. The measured data is shown in Fig. 3 together with the available literature data and the theoretical data from the model code calculations. The two maximums at around 12 MeV and 29 MeV are from the independent contributions of the $^{114}\text{Cd}(p, n)$ and $^{116}\text{Cd}(p, 3n)$ reactions, respectively. We found a good overall agreement with the Tarkanyi et al. [1] and Nortier et al. [9] reported data but the data reported by Zaitseva et al. [10] revealed a discrepancy due to a significant energy shift. The TALYS code reproduced a nicely fitted excitation function with the measured ones, whereas the ALICE-IPPE code produced a similar shape but overestimated the magnitudes.

4.4 The $^{nat}\text{Pd}(p,x)^{105}\text{Rh}$ processes

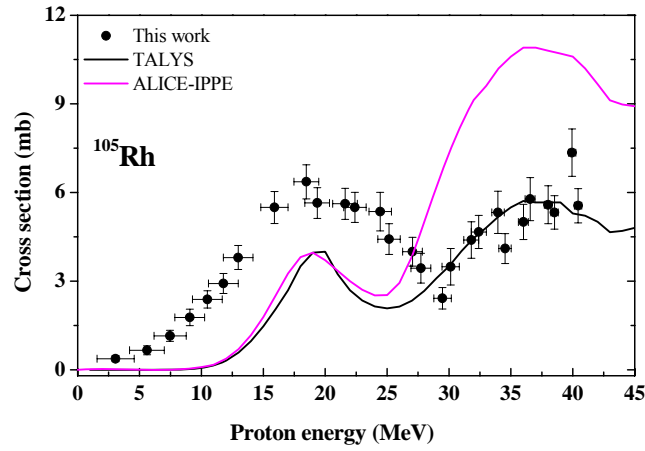


Fig. 4 Excitation function for the $^{nat}\text{Pd}(p,x)^{105}\text{Rh}$ processes

The long-lived radionuclide ^{105}Rh ($T_{1/2}=1.47$ d) has a short-lived meta-stable state ^{105m}Rh ($T_{1/2}=40.0$ s), which completely decays to its ground state by an IT process before starting our measurement. Therefore, the formation of the ^{105}Rh radionuclide follows a cumulative process. The radionuclide ^{105}Rh was identified using its strong and independent gamma line, $E_\gamma = 318.9$ keV ($I_\gamma=19.1\%$). The direct contributing channels for the formation of this radionuclide are the $^{106}\text{Pd}(p, 2p)$, the $^{108}\text{Pd}(p, \alpha)$ and the $^{110}\text{Pd}(p, 2n\alpha)$ reactions. We couldn't compare the present results with any previous measurements due to the lack of available literature data. The measured excitation function of this radionuclide formation is shown in Fig. 4 and compared with the value predicted from the TALYS and the ALICE-IPPE codes, and we found a partial agreement with the TALYS prediction above 30 MeV whereas ALICE-IPPE overestimates it in this energy region.

5. Integral yield

The integral yields were deduced using the measured cross-sections of the radionuclides over the energy range from their threshold to 40 MeV by taking into account that the total energy is absorbed in the targets. The deduced yields are expressed as $\text{MBq}\cdot\mu\text{A}^{-1}\cdot\text{h}^{-1}$, and are presented in Fig. 5.

6. Conclusions

Production cross-sections for the $^{nat}\text{Cd}(p,x)^{109g,111g,114m}\text{In}$ and $^{nat}\text{Pd}(p,x)^{105}\text{Rh}$ nuclear processes have been reported from 40 MeV down to their threshold energy with an overall uncertainty of about 15%. Standardization and validation of the measured data were done using the available literature data, and the theoretical data from the TALYS and ALICE-IPPE codes. The present measured cross-sections of ^{111}In from a natural cadmium target could be used for a validation of the IAEA recommended data. But, the production of this radionuclide from a natural cadmium target is not suitable due to a contamination from a simultaneously produced ^{114m}In radionuclide in our investigated energy range. However, highly enriched $^{111,112}\text{Cd}$ targets could be used to obtain a suitable production of the ^{111}In radionuclide with a minimum impurity level. On the other hand, the deduced thick target yield showed that a low energy (<20 MeV) medical cyclotron and highly enriched $^{108,110}\text{Pd}$ targets could be used for a profitable production of ^{105}Rh with a minimum impurity from ^{101m}Rh , even though under the above conditions the production of a ^{101m}Rh impurity is not possible, energetically. Above all, the present investigation is the first report on a cyclotron production of a carrier free ^{105}Rh radionuclide as an alternative route to the currently used neutron activation process by a nuclear reactor. In addition, the present experimental results will play an important role in the enrichment of the literature data base for the $^{nat}\text{Cd}(p,x)^{109g,111g,114m}\text{In}$ and $^{nat}\text{Pd}(p,x)^{105}\text{Rh}$ nuclear processes leading to various applications.

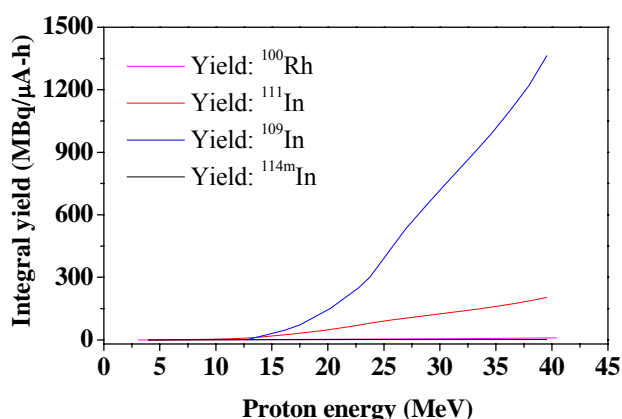


Fig. 5 Integral yields for the ^{100}Rh and $^{109g,111g,114m}\text{In}$ radionuclides

Acknowledgments

This work was partly supported by the Korea Science and Engineering Foundation (KOSEF) through a grant provided by the Korean Ministry of Education, Science and Technology (MEST) in 2008 (Project No. 08M040001110), and by the Science Research Center project through the Center for High Energy Physics, Kyungpook National University.

References

- [1] F. Tarkanyi et al., Nucl. Instr. and Meth., B **245**, 379 (2006).
- [2] M.L. Thakur, A.D. Nunn, Int. J. Appl. Radiat. Isot., **23**, 139 (1972).
- [3] W.J. Nieckarz, A.A. Caretto, Phys. Rev., **178**(4), 1887 (1969).
- [4] J. Zweit, Phys. Med. Biol., **41**, 1905 (1996).

- [5] R.C. Brooks et al., Nucl. Med. Biol., **26**, 421 (1999).
- [6] S. M. Qaim, Radiat. Phys. and Chem., **71**, 917 (2004).
- [7] D. E. Troutner, Int. J. Radiat. Appl. Inst., Part B. Nucl. Med. Biol., **14**, 171 (1987).
- [8] F. Ta'rká'nyi et al., Radiochim. Acta, **93**, 1 (2005).
- [9] F.M. Nortier et al., Appl. Radiat. Isot., **41**, 1201 (1990).
- [10] N.G. Zaitseva et al., Appl. Radiat. Isot., **41**, 177 (1990).
- [11] S.M. Kormali et al., J. Radioanal. Chem., **31**, 437 (1976).
- [12] F. Ditrói et al., [J. Radioanal. Nucl. Chem.](#), **272(2)**, 231 (2007).
- [13] M.U. Khandaker et al., Nucl. Instr. and Meth. B, **262**, 171 (2007).
- [14] F. Tarkanyi et al., IAEA-TECDOC-1211, Available from <<http://www-nds.iaea.org/medical/>>.
- [15] J.F. Ziegler et al., SRIM 2003 code, Available from <<http://www.srim.org/>>.
- [16] NUDAT data base, Available from <<http://www.nndc.bnl.gov/nudat2/>>
- [17] A.J. Koning et al., TALYS: Comprehensive nuclear reaction modeling, in *Proc. Int. Conf. Nucl. Data for Sci. and Tech.- ND2004*, Santa Fe, USA, AIP vol. **769**, p.1154, 2005.
- [18] A.I. Dityuk et al., New Advanced Version of Computer Code ALICE-IPPE, INDC (CCP) - 410, IAEA, Vienna, 1998.: MENDL-2P, <<http://www-nds.iaea.org/nucmed.html>>.
- [19] S. Takacs et al., Nucl. Instr. and Meth., B **240**, 790 (2005).